

## Dislocation loops in overheated free-standing smectic films

A. N. Shalaginov and D. E. Sullivan

*Department of Physics and Guelph-Waterloo Physics Institute, University of Guelph, Guelph, Ontario, Canada N1G 2W1*

(Received 31 May 2001; revised manuscript received 8 November 2001; published 1 March 2002)

Static and dynamic phenomena in overheated free-standing smectic-*A* films are studied theoretically. The work is based on a generalization, introduced recently by the authors, of de Gennes' theory for a confined presmectic liquid. In this approach, smectic ordering in an overheated film is caused by an intrinsic surface contribution to the film free energy and vanishes at some temperature depending on the number of layers. Here the theory is further generalized to study the dynamics of films with planar inhomogeneities. A static application is to determine the profile of the film meniscus and the meniscus contact angle, the results being compared with those of a recent study employing de Gennes' original theory. The dynamical generalization of the theory is based on a time-dependent Ginzburg-Landau approach. This is used to compare two modes for layer-thinning transitions in overheated free-standing films, namely, "uniform thinning" versus nucleation of dislocation loops. It is concluded that the nucleation mechanism dominates provided there is a sufficiently large pressure difference arising from meniscus curvature. Properties such as the line tension and velocity of a moving dislocation line are evaluated self-consistently by the theory.

DOI: 10.1103/PhysRevE.65.031715

PACS number(s): 61.30.Jf, 64.60.Ht, 64.70.Md

### I. INTRODUCTION

Free-standing films of several smectic-*A* liquid-crystalline compounds can be heated above the bulk smectic disordering temperature without immediately rupturing, and instead are found to undergo successive layer-by-layer thinning transitions as the temperature is increased [1–6]. The persistence of smectic layering in an overheated thin film is usually attributed to enhanced ordering associated with the free surfaces of the film, as is known to occur in other contexts [7]. There is not yet, however, a clear consensus on the mechanisms by which layer thinning occurs. According to one set of theories [8–11], thinning takes place when the smectic layer structure throughout the middle of a film vanishes. In an alternative theory [12], supported by experimental studies [13], layer thinning occurs by spontaneous nucleation of dislocation loops prior to the melting of the layer structure in the film interior.

One of the key experimental observables is the variation of layer-thinning transition temperatures  $T_c(N)$  with the number of film layers  $N$ , which is found to be well fit by the power-law relation  $N \propto t^{-\nu}$ , where  $t = (T_c(N) - T_0)/T_0$ ,  $\nu \approx 0.70 \pm 0.10$ , and  $T_0$  is close to the bulk transition temperature. Alternative mathematical relations [10,12,14] and an upper bound [11] for  $T_c(N)$  have been derived from the different theories. With appropriate fitting parameters, these alternative relations all turn out to agree well with the power-law expression and, thus, are not able to distinguish between the various mechanisms.

In this paper, we examine further the connections between the different proposed mechanisms of layer-thinning transitions. As in several recent works [10,12,14], our analysis is based on de Gennes' [15] phenomenological Landau theory for a "presmectic" film of a fluid exhibiting a *second-order* bulk smectic-*A* to nematic ( $N$ ) transition. More precisely, we employ a generalization of that theory recently proposed by the present authors [11]. One drawback of de Gennes' original model stems from attributing surface-enhanced

smectic ordering to an external-field-like coupling term of constant magnitude, which is more appropriate for a film confined between solid walls. This has the consequence that a weak degree of smectic ordering in a thin film is predicted to persist up to arbitrarily high temperatures. In order to induce layer thinning, recent studies based on this theory have included the effects of a pressure difference  $\Delta P$  associated with curvature of the meniscus at the film border [10,14]. According to the latter studies,  $\Delta P$  must be of a sufficient magnitude to cause layer thinning, although the layer-thinning transition temperatures are predicted to depend only logarithmically on  $\Delta P$ . The modified version of de Gennes' theory proposed by the present authors [11] utilizes a different form of the surface contribution to the free energy (suggested by older theories of wetting [16]), which is quadratic rather than linear in the surface order parameter and which restores smectic melting at high temperatures without requiring the pressure term.

According to the theory of Ref. [11], reviewed here in Sec. II, the free energy per unit area of an overheated smectic film exhibits a discrete sequence of metastable local minima, whose depths decrease with increasing number of layers up to some finite maximum  $N_{cr}$  depending on temperature. At or slightly below the temperature for which the free-energy well at  $N_{cr}$  vanishes, it was assumed in Ref. [11] that the film would spontaneously thin down to a smaller thickness. This assumption makes no statement on "how" layer thinning occurs, which is the question addressed in this paper. We proceed by generalizing the theory to allow for inhomogeneities in the film thickness (Sec. III) as well as the dynamical evolution of the film, using a time-dependent Ginzburg-Landau approach (Sec. IV). In the static limit, the theory provides a description of the contact angle between the film and meniscus, which we compare with the recent experimental and theoretical studies of Picano *et al.* [14]. Using the dynamical theory, we investigate the nucleation of dislocation loops between film domains of different thicknesses and the subsequent growth of the thinner region of the film,

which is contrasted with the “uniform-thinning” mechanism for the film to achieve a state of lower free energy. The results are mapped onto the conventional nucleation picture, in which the activation free-energy barrier to nucleation depends on both the difference in well depths of the homogeneous film regions and the line tension  $E$  of the dislocation loop. Here we calculate the line tension  $E$ , activation energy, and velocity of a growing loop self-consistently in the dynamical model, and evaluate their dependence on temperature and number of layers. It is found that thinning via nucleation of dislocation loops preempts the uniform-thinning mechanism provided the pressure difference  $\Delta P$ , due to the meniscus, is sufficiently large. Further discussion of our findings, their relation to those of previous studies, and the fact that they are restricted to smectic systems with continuous as opposed to first-order bulk transitions, are discussed in Sec. V.

## II. THEORY OF UNIFORM FILMS

In this section, we review the generalized de Gennes theory in the case of a uniform planar free-standing smectic film: further details can be found in Ref. [11]. The film is modeled by a thin liquid slab bounded by two parallel surfaces located at  $z = \pm L/2$ , where  $L$  is the film thickness. The degree of smectic order in the film is represented by the complex order parameter  $\Psi(z)$ , where the real part of  $\Psi(z)\exp(iq_0z)$  describes spatial modulation of the density. Here  $q_0 = 2\pi/d$ , with  $d$  being the unstressed smectic layer spacing. The order parameter is parametrized as

$$\Psi(z) = \psi(z)\exp[-i\phi(z)], \quad (1)$$

where  $\psi(z)$  is the amplitude and  $\phi(z) \equiv q_0 u(z)$  is a phase proportional to the layer displacement  $u(z)$ .

The Landau free energy per unit area of the film [17] is taken to be

$$f = \frac{1}{2} \int_{-L/2}^{L/2} dz \left[ r\psi^2 + \frac{1}{2}g\psi^4 + C(\nabla_z\psi)^2 + C\psi^2(\nabla_z\phi)^2 \right] + \frac{1}{2}r_s[\psi^2(L/2) + \psi^2(-L/2)] - h_s[\psi(L/2) + \psi(-L/2)], \quad (2)$$

where  $C$  is an elastic constant and  $h_s, r_s$  are coupling constants associated with surface interactions. The bulk free-energy density  $(r\psi^2 + g\psi^4/2)/2$  in Eq. (2), with  $g > 0$ , is strictly applicable only to a system exhibiting a second-order smectic-nematic transition. We express  $r = a(T - T^*)$ , where  $T^*$  denotes the bulk mean-field transition temperature. Euler-Lagrange equations determining  $\psi(z)$  and  $\phi(z)$  are obtained by functional minimization of Eq. (2) [11]. In addition, it is assumed that the film contains an integral number of layers  $N$ , which fixes [15] the surface value of the phase  $\phi(L/2) = \pi(L/d - N)$ .

Following the original work of de Gennes [15], several previous studies of surface-enhanced ordering of free-standing smectic films using this theory have attributed such

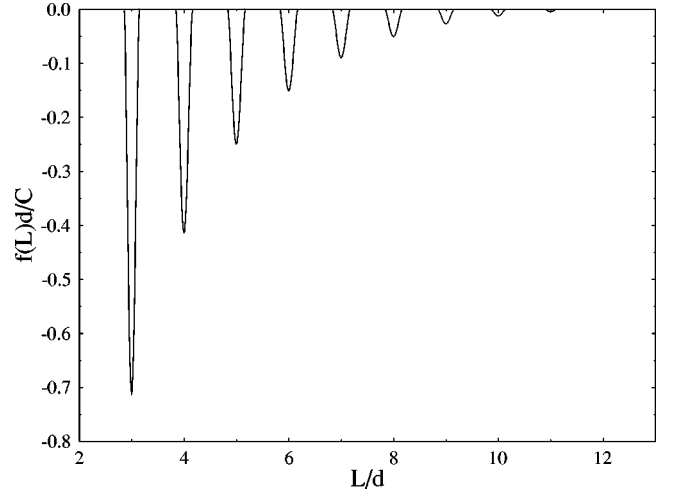


FIG. 1. Dimensionless free energy per unit area  $fd/C$  vs thickness  $L/d$  calculated using scaled parameters  $h_s=0$ ,  $r_s d/C = -0.2$ ,  $gd^2/C = 0.01$ , and  $rd^2/C = 0.05$ .

ordering solely to the surface field  $h_s$ , with  $r_s = 0$  [10,12,14]. These studies have also set the parameter  $g = 0$ , thereby restricting consideration to the overheated regime  $T > T^*$ . Under the condition  $g = 0$ , an analytic solution of the theory is easily obtained [15]. It is found that the smectic amplitude  $\psi(z)$  decays exponentially with distance from the surfaces at  $z = \pm L/2$  and tends toward a small value in the middle of the film. The phase  $\phi(z)$  is nonzero when the film thickness  $L$  differs from an integral multiple of  $d$ , and exhibits its largest gradient  $|\nabla_z\phi|$  in the middle of the film. One drawback of this model, a consequence of neglecting the quartic term  $g\psi^4$  in Eq. (2), is that the resulting equilibrium free energy  $f(L)$  and the order parameter  $\psi(z)$  throughout the film diverge on approaching the bulk transition temperature  $T^*$ , as is shown by the expressions for these quantities given in previous work [10,12,14,15].

In Ref. [11], smectic ordering in an overheated film is attributed to a nonzero value  $r_s < 0$ , with  $h_s = 0$ . In the following, we refer to this as the  $r_s$  model. In this case, the Euler-Lagrange equations following from Eq. (2) always admit a trivial solution  $\psi(z) = 0$ , representing a nematic state of the film, which is the only solution existing at sufficiently high temperature. The numerical solution of those equations is described in Ref. [11] for the general case  $g \neq 0$ . The variation of the equilibrium free energy  $f(L)$  typical for this model is depicted in Fig. 1. The free energy exhibits a set of wells with centers situated approximately at  $L = Nd$  and depths diminishing with  $N$ , while  $f(L)$  vanishes over wide ranges of  $L$  between the wells. In the latter ranges of  $L$ , where  $f(L) = 0$ , the order parameter  $\psi(z)$  is identically zero. Although not discernable in the figure, the slope of the free energy smoothly approaches zero at the limits where  $f(L) \rightarrow 0$ . In the temperature range  $T < T_s$ , where  $T_s = T^* + r_s^2/(Ca)$ ,  $f(Nd)$  for all  $N$  is smaller than some negative threshold depending on  $T$ . On the other hand, for temperatures  $T > T_s$ , wells with nonzero depths occur only for  $N \leq N_{cr}$ , where  $N_{cr}$  is finite and depends on  $T$ . This in the case in Fig. 1, where  $N_{cr} = 11$ . It was argued in Ref. [11] that the

temperature at which the free-energy well for  $L = N_{cr}d$  disappears, which we will call the “maximum temperature” for an  $N_{cr}$ -layer film, is an upper limit for the layer-thinning transition temperature  $T_c(N_{cr})$ . Films of all  $N < N_{cr}$  can still exist as metastable states and, in principle, thinning could then occur to any one of these states. In contrast, we note that the original version of de Gennes’ presmectic model [10,12,14,15], with  $r_s = 0$ , predicts that a weakly ordered smectic state of the film exists and is more stable than the disordered state at all temperatures  $T > T^*$ .

The following scaling of the  $r_s$  model free energy is used in Fig. 1 and in subsequent analyses. On expressing distances in units of the layer spacing  $d$ , the free energy in Eq. (2) can be expressed as  $f(L, r, g, r_s, C) = (C/d)\hat{f}(L/d, \hat{r}, \hat{g}, \hat{r}_s)$ , where  $\hat{r} = rd^2/C$ ,  $\hat{g} = gd^2/C$ , and  $\hat{r}_s = r_s d/C$ . While an additional scaling transformation of the order parameter  $\psi$  could be applied to factor out the parameter  $\hat{g}$  from  $\hat{f}$ , we have found it convenient for numerical analysis to set this at the (arbitrary) value  $\hat{g} = 0.01$  and leave the scaling of  $f$  in the form indicated.

### III. NONUNIFORM FILMS: STATICS

In order to study the growth of dislocation loops and associated phenomena in free-standing films, the theory of Sec. II should be generalized to account for inhomogeneities in the film thickness  $L$ . Here we treat this problem by a Landau approach of expanding the film free energy in powers of gradients of  $L$ , yielding an “effective interface” theory [19]. We will assume that the film is symmetrical about its mid-plane at  $z = 0$ , so that its top and bottom surfaces do not vary independently. To lowest order in gradients of  $L$ , the total film free energy is then given by

$$F = \int d^2r_{\perp} \left[ \tilde{f}(L) + \frac{1}{2} D (\nabla_{\perp} L)^2 \right], \quad (3)$$

where the horizontal or in-plane direction is denoted  $\mathbf{r}_{\perp}$ , having Cartesian components  $(x, y)$ ,  $\nabla_{\perp} = (\nabla_x, \nabla_y)$ , and  $L = L(\mathbf{r}_{\perp})$  is the spatially varying film thickness. The function  $\tilde{f}(L)$  is the equilibrium free energy per unit area of a film of *uniform* thickness  $L$ : as discussed shortly, this may differ slightly from the equilibrium free energy  $f(L)$  obtained from Eq. (2).

One contribution to the coefficient  $D$  in Eq. (3) is given by  $\gamma/2$ , resulting from the liquid-air interfacial tension  $\gamma$  of the free surfaces bounding the film. While this surface contribution could vary with  $L$  due to changes in the degree of smectic ordering, such effects should be small compared with that due to the liquid-air density difference across the interfaces. On setting  $D = \gamma/2$ , the free energy in Eq. (3) agrees with the small  $(\nabla_{\perp} L)$  limit [20] of that used in Ref. [14] to analyze the shape of the meniscus at the edge of a free-standing film. In addition, contributions to  $D$  arising from horizontal gradients of the order parameter  $\Psi$  and nematic director  $\hat{\mathbf{n}}$  in the film interior may be present. In principle, the latter contributions could be determined by generalizing the free energy of Eq. (2) to include such gradient

terms, consistent with de Gennes’ more general theory of the  $N$ -A transition [23], and expanding the solutions of the corresponding Euler-Lagrange equations for  $\Psi$  and  $\hat{\mathbf{n}}$  in powers of the gradients of  $L$ . These elastic effects, however, are also expected to be small compared with those from  $\gamma$  in the case of an overheated film due to the weak degree of smectic ordering in the middle of a film. This is also consistent with arguments given in Ref. [10]. (We note that the model free energy considered in Ref. [14], following earlier work in Ref. [21], included an additional term attributed to the energy of edge dislocations, but this contribution was found to vanish under integration and plays no role in film statics [22].) Finally, higher-order gradient terms (i.e.,  $(\nabla_{\perp} L)^4$ ,  $(\nabla_{\perp}^2 L)^2$ , etc.) should also occur in the free energy  $F$ , but these will be omitted here on assuming that the gradient and curvature of  $L$  are small [20].

The function  $\tilde{f}(L)$  may differ from  $f(L)$  of Eq. (2) due to the existence of a positive pressure difference  $\Delta P = P_{air} - P_{liquid}$  across the surface of the meniscus surrounding the film. Such a pressure difference would produce a shift  $\Delta\mu$  in the chemical potential of the film molecules from their value at coexistence with the vapor phase across a planar interface [24,25]. This leads to

$$\tilde{f}(L) = f(L) + \Delta PL. \quad (4)$$

The main effect of the  $\Delta P$  term is to shift the depths and to a slight extent the positions of the smectic minima of the effective free energy  $\tilde{f}(L)$  with respect to those of  $f(L)$ , possibly eliminating minima occurring at large  $L$  [10].

Here we will use the static free energy [Eq. (3)] with  $\tilde{f}(L)$  given by Eq. (4), to analyze the meniscus shape. This closely follows the analysis of Ref. [14], although the latter work was based on de Gennes’ original model for  $f(L)$ , while here we will employ the  $r_s$  model with  $g \neq 0$ . The profile of the meniscus is found by minimizing Eq. (3) with respect to  $L$ , subject to the boundary condition that the bulk of the film has a thickness  $L \equiv H \approx Nd$ . Assuming that  $L$  varies only in the  $x$  direction and  $D$  is independent of  $L$ , the resulting Euler-Lagrange equation is

$$D \frac{d^2 L}{dx^2} - \frac{\partial \tilde{f}}{\partial L} = 0. \quad (5)$$

The first integral of this equation, with the boundary condition  $L(-\infty) = H$ , is

$$\frac{D}{2} \left( \frac{dL}{dx} \right)^2 = \tilde{f}(L) - \tilde{f}(H), \quad (6)$$

which has the implicit solution

$$x = \sqrt{\frac{D}{2}} \int_{L(0)}^{L(x)} dL' [\tilde{f}(L') - \tilde{f}(H)]^{-1/2}. \quad (7)$$

Here both the origin  $x = 0$  and the corresponding value  $L(0) > H$  are arbitrary. Related considerations have been applied to describe the shape of liquid droplets on a solid sub-

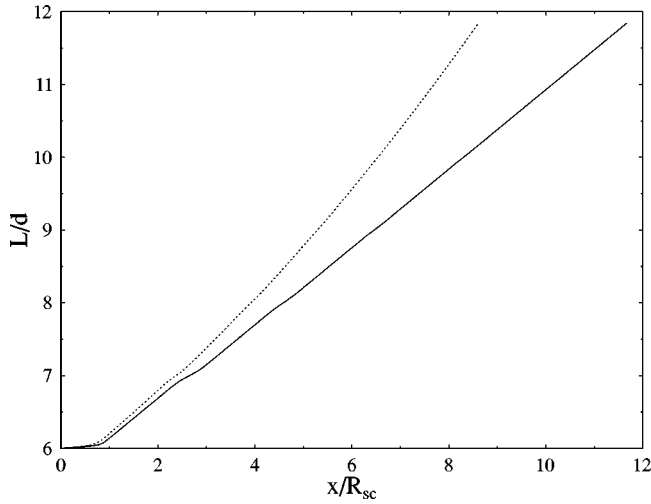


FIG. 2. Thickness of the meniscus vs scaled in-plane distance  $x/R_{sc}$ , using the  $f(L)$  function of Fig. 1. The solid line corresponds to  $\Delta P=0$  while the dotted line corresponds to  $\Delta P=0.05C/d^2$ . The origin  $x=0$  is such that, for both curves,  $L(x=0)=6.00001$ .

strate [26,27]. However, the description based on the above equations is only valid for small  $|\nabla_{\perp} L|$ ; deep in the meniscus, higher-order terms in  $\nabla_{\perp} L$  [20] may be needed for an accurate treatment.

Figure 2 shows the solutions to Eq. (7) for the  $r_s$  model using the same parameters as in Fig. 1. Two cases are shown, the solid line corresponding to  $\Delta P=0$  while the dotted line corresponds to  $\Delta P=0.05C/d^2$ . The reduced unit for  $\Delta P$  is consistent with that for  $f$  discussed at the end of Sec. II. Following from that scaling and Eq. (7), the horizontal distance  $x$  is expressed in units of  $R_{sc} \equiv d\sqrt{Dd/C}$ . In both cases, the meniscus profile is seen to be fairly smooth, rather than exhibiting the clear separation of distinct steps of height  $\approx d$  expected [21,25] at low temperatures when the smectic- $A$  phase is stable in bulk. The smoothness of the meniscus profiles in Fig. 2 is a consequence of being in the overheated regime.

For  $T < T_s$ , the function  $f(L)$  tends to a nonzero value  $f(\infty)$  with increasing  $L$ . The latter represents the contribution of surface-induced smectic ordering to twice the interfacial tension  $\gamma$  of the liquid-vapor interface of a semi-infinite liquid. Neglecting small oscillations of  $f(L)$  about  $f(\infty)$  and defining the meniscus slope angle  $2\theta \approx dL/dx$ , Eqs. (6) and (4) lead to

$$\theta^2 = \frac{1}{2D} [f(\infty) - f(H) + \Delta P(L - H)]. \quad (8)$$

On assuming that  $D = \gamma/2$  and extrapolating the function in Eq. (8) down to  $L=H$ , we obtain for the contact angle  $\theta_m$  between the meniscus and film,

$$\theta_m^2 = \frac{1}{\gamma} [f(\infty) - f(H)], \quad (9)$$

independent of  $\Delta P$ . This result agrees with that derived in Ref. [14]; we note that essentially equivalent relations were

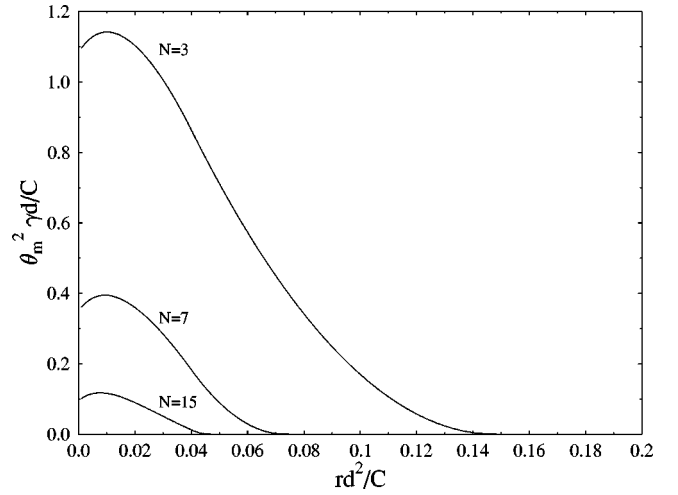


FIG. 3. Squared meniscus contact angle  $\theta_m^2$  in units of  $C/\gamma d$  as a function of dimensionless temperature variable  $rd^2/C \propto (T - T^*)$  for various number of layers  $N$ , calculated in the  $r_s$  model with the same parameters as in Fig. 1.

derived some time ago in the case of soap films [24,28]. Note also that Eq. (8) predicts growth of  $\theta$  with increasing  $L$  for  $\Delta P > 0$ . The meniscus curvature  $\kappa$  is found to be

$$\kappa \equiv \frac{d\theta}{dx} = \frac{d\theta}{dL} \frac{dL}{dx} = \frac{d\theta^2}{dL} = \frac{\Delta P}{\gamma}, \quad (10)$$

which is just the Laplace law.

Using the original de Gennes model ( $g=r_s=0$ ) free energy, we find that the contact angle diverges as  $T$  approaches  $T^*$  from above, whereas the experimental results of Ref. [14] indicate regular behavior in this region. The calculations of Ref. [14], based on the same model but fixing  $\psi(L/2)$  instead of  $h_s$ , predicted a different anomaly in the contact angle, namely, that  $\theta_m$  vanishes as  $T \rightarrow T^*$  for all  $N$ . The divergence of the contact angle near the bulk second-order transition in the original de Gennes model is removed by setting  $g \neq 0$ . Here we present results for  $\theta_m$  using the  $r_s$  model, although qualitatively similar results are obtained using  $r_s=0$  with  $h_s \neq 0$  and  $g \neq 0$ . Figure 3 shows  $\theta_m^2$ , in units of  $C/(d\gamma)$ , as a function of  $\hat{r} \propto (T - T^*)$  for various number of layers  $N$ , using the free energy  $f(L)$  depicted in Fig. 1. It is seen that  $\theta_m$  remains nonzero on approaching the bulk transition temperature and increases with decreasing  $N$ , in agreement with experiment [14]. We also find that the contact angle vanishes above the maximum temperature for a given number of layers. This is in contrast with the model of Ref. [14], which yields a small but nonzero contact angle for arbitrarily large temperature and film thickness. However, as seen in Fig. 3, the maximum in  $\theta_m$  as a function of temperature is fairly insensitive to the number of layers, which does not accord with the experimental results.

Comparison of Fig. 3 with the experimental data [14] for  $\theta_m^2$  indicates that the scaling unit  $C/(d\gamma)$  should be of the order of  $10^{-2}$ . Taking  $D = \gamma/2$ , we then estimate the in-plane distance scale unit to be  $R_{sc} \equiv d\sqrt{Dd/C} \approx (10/\sqrt{2})d \approx 2$

$\times 10^{-8}$  m, where we have used the value  $d = 3 \times 10^{-9}$  m [22]. This estimate will be utilized in calculations described in the following section.

#### IV. DYNAMICS OF NONUNIFORM FILMS

##### A. Time-dependent Ginzburg-Landau equation

Now we extend the theory of the preceding section to account for the dynamics of thickness variations. We will focus on dynamical processes with large enough characteristic times to neglect inertial effects. Although the details of relaxation are undoubtedly quite complicated, here we will proceed by assuming the simplest possible dissipative dynamics for  $L$ , based on a time-dependent Ginzburg-Landau (TDGL) equation [29]. This equation is appropriate for describing the dynamics of a nonconserved variable, which  $L$  can be regarded in the case of a film open to the exchange of molecules with the meniscus. The TDGL equation is

$$\eta \frac{\partial L}{\partial t} = - \frac{\delta F}{\delta L} = \left[ D \nabla_{\perp}^2 L - \frac{\partial \tilde{f}}{\partial L} \right]. \quad (11)$$

Here  $\delta F / \delta L$  is the functional derivative of the film free energy  $F$ , given by Eq. (3), providing the thermodynamic force that drives the system toward equilibrium,  $t$  is time, and  $\eta$  is a kinetic coefficient that we will assume to be constant. As in the preceding section, we have assumed  $D$  to be independent of  $L$ .

Two opposing mechanisms for thinning of an overheated smectic film are “uniform thinning” (i.e., with  $\nabla_{\perp} L = 0$  for all  $\mathbf{r}_{\perp}$ ) and via nucleation of dislocation loops. If the initial film thickness  $L_0 \equiv L(t=0) \approx Nd$  is *uniform* and at a local minimum of the shifted free energy  $\tilde{f}$ , then it will remain so indefinitely according to Eq. (11). (This picture neglects possible disruption due to thermal fluctuations, which we neglect in this paper.) Under small displacements of the thickness from the initial value  $L_0$ , the film will be restored to that initial thickness. Hence uniform thinning can only occur at the maximum temperature of an  $N$ -layer film, and then only if  $\Delta P > 0$  [30].

To examine the growth of dislocation loops, for simplicity we first consider a one-dimensional solution of Eq. (11), in the form of an infinite straight-line kink parallel to the  $y$  axis separating domains of thicknesses  $L_1$  and  $L_2$  and moving in the  $x$  direction, illustrated in Fig. 4,

$$L = \Phi(x - v_{\infty} t), \quad (12)$$

where the function  $\Phi$  and kink velocity  $v_{\infty}$  are to be determined. Substituting Eq. (12) into Eq. (11) yields the ordinary differential equation

$$D \Phi'' + \eta v_{\infty} \Phi' - \frac{\partial \tilde{f}(\Phi)}{\partial \Phi} = 0, \quad (13)$$

with boundary conditions

$$\Phi(-\infty) = L_1, \quad (14a)$$

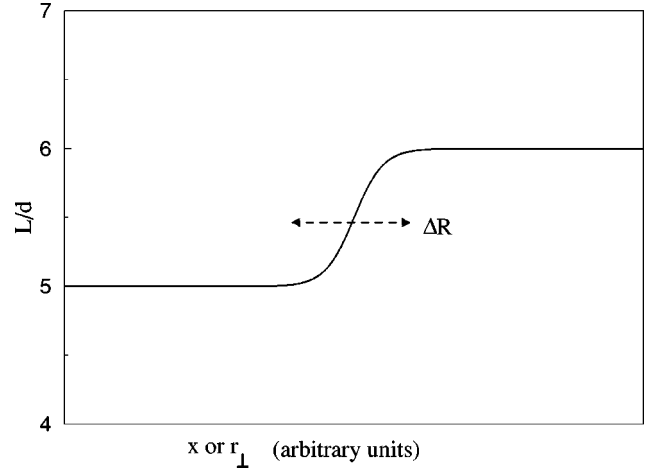


FIG. 4. Schematic picture of the film thickness variation for a step separating five-layer and six-layer domains. The horizontal coordinate is either  $x$  or  $r_{\perp}$ , corresponding to one-dimensional or two-dimensional motion of the kink, respectively. The width of the kink is represented by  $\Delta R$ .

$$\Phi(\infty) = L_2, \quad (14b)$$

where the prime symbols ( $'$ ) denote derivatives of  $\Phi$  with respect to its argument. The thicknesses  $L_1$  and  $L_2$  are at local minima of  $\tilde{f}(L)$ . Usually, we will take these to be adjacent minima, with  $L_1 \approx (N-1)d$ ,  $L_2 \approx Nd$ , and  $\tilde{f}(L_1) < \tilde{f}(L_2)$ .

Equation (13) has a well-known mechanical analogy [31,32]. It can be considered as the dynamical equation describing movement of a particle of “mass”  $D$  in a medium with “friction coefficient”  $\eta v_{\infty}$  and subject to a “potential energy”  $-\tilde{f}(L)$ . That equation has no stationary solution ( $v_{\infty} = 0$ ) unless the depths of the minima of  $\tilde{f}(L)$  at  $L_1$  and  $L_2$  are equal. This follows by considering the first integral of Eq. (13), namely,

$$\frac{d}{dX} \left[ \frac{1}{2} D (\Phi')^2 - \tilde{f}(\Phi) \right] = - \eta v_{\infty} (\Phi')^2, \quad (15)$$

where  $X \equiv x - v_{\infty} t$  is the argument of  $\Phi$ . Integrating Eq. (15) over  $X$  using the boundary conditions Eq. (14) yields

$$v_{\infty} = \frac{D}{\eta E} [\tilde{f}(L_2) - \tilde{f}(L_1)], \quad (16)$$

where the quantity  $E$  is defined as

$$E \equiv D \int_{-\infty}^{\infty} dX (\Phi')^2 = D \int_{L_1}^{L_2} d\Phi \Phi'. \quad (17)$$

Equation (16) shows that  $v_{\infty}$  is proportional to the free-energy difference  $\tilde{f}(L_2) - \tilde{f}(L_1)$  and, hence, vanishes if that difference is zero. As discussed in the following section,  $E$  can be identified with the line tension of the dislocation loop.

For any function  $\tilde{f}(L)$  characterized by two unequal adjacent minima, as is the case here, there should be a unique

solution of Eq. (13) for the velocity  $v_\infty > 0$  and function  $\Phi$  describing the profile of the kink, which moves toward the region of thickness  $L_2$  in order to eliminate the domain of higher free energy. Under conditions where the higher minimum of  $\tilde{f}(L)$  at  $L_2$  vanishes and becomes a point of zero curvature, as happens in the present model at the maximum temperatures, the velocity  $v_\infty$  and kink shape may become nonunique. In other contexts [31,33,34], this is called a state of marginal stability. Here, we always find (Sec. IV C) that uniform thinning occurs under these conditions when  $\Delta P > 0$  [30].

The solutions of the one-dimensional equation Eq. (13) turn out to be relevant in the more general two-dimensional case, as discussed in the following subsection.

### B. Nucleation of dislocation loops

If a dislocation loop separating  $N$ - and  $(N-1)$ -layer regions is nucleated, initially it will be of finite size. According to the conventional nucleation picture (see, e.g., Refs. [12,21,23] for the case of smectic films), the loop then will either expand or collapse depending on whether its initial radius is greater or smaller than some ‘‘critical’’ value. Here we are interested in determining the critical radius, the associated activation free energy, and the subsequent dynamical evolution of the loop.

We assume that the dislocation loop is a circle, as observed in recent experiments [12,13]. Using in-plane polar coordinates, with origin at the center of the loop and radial distance denoted  $r_\perp$ , Eq. (11) becomes

$$\eta \frac{\partial L}{\partial t} = \left[ D \frac{1}{r_\perp} \frac{\partial}{\partial r_\perp} \left( r_\perp \frac{\partial L}{\partial r_\perp} \right) - \frac{\partial \tilde{f}}{\partial L} \right]. \quad (18)$$

The associated boundary conditions are

$$\left( \frac{\partial L(r_\perp)}{\partial r_\perp} \right)_{r_\perp=0} = 0, \quad (19a)$$

$$L(\infty) = L_2 \approx Nd. \quad (19b)$$

The film thickness in the center of the loop at  $r_\perp = 0$  will usually be close to the value  $L_1 \approx (N-1)d$ . The change in free energy due to formation of the loop is

$$\begin{aligned} \Delta F &= \frac{1}{2} \int d^2 r_\perp [2\tilde{f}(L) - 2\tilde{f}(L_2) + D(\nabla_\perp L)^2] \\ &= \pi \int_0^\infty dr_\perp r_\perp \left[ 2\tilde{f}(L) - 2\tilde{f}(L_2) + D \left( \frac{\partial L}{\partial r_\perp} \right)^2 \right]. \quad (20) \end{aligned}$$

In the case of a stationary solution of Eq. (18), corresponding to a ‘‘critical’’ nucleus,  $\Delta F$  is the activation free energy.

The profile of  $L(r_\perp)$  describing a dislocation loop should have a kink structure, as in Fig. 4, with  $\partial L / \partial r_\perp \approx 0$  everywhere except within a narrow region of width  $\Delta R$  centered around some value  $r_\perp = R$ . Numerical solution of the stationary limit of Eq. (18), with  $(\partial L / \partial t) = 0$  and the boundary conditions Eq. (19) is difficult, precisely because this is as-

sociated with a unique ‘‘critical’’ value of the loop radius  $R$ . We have found it more expedient, and of more general relevance, to solve the full time-dependent partial differential equation (18), using a standard subroutine (NAG FORTRAN D03PCF). Our results reported below in Sec. IV C have been obtained from this numerical analysis. However, we have found that those results are very well reproduced using the following ansatz for  $L(r_\perp, t)$ , having the form of a moving kink:

$$L(r_\perp, t) = \Phi[r_\perp - R(t)]. \quad (21)$$

As discussed some time ago in a general context by Chan [35], this form is not an exact solution of the two-dimensional equation (18) but should be a good approximation if the kink radius  $R$  is much larger than its width  $\Delta R$ . On substituting Eq. (21) into Eq. (18) and approximating  $1/r_\perp$  by  $1/R$ , we arrive again at the *one-dimensional* equation (13), but with  $v_\infty$  defined as [35]

$$v_\infty = \frac{dR}{dt} + \frac{D}{\eta} \frac{1}{R}. \quad (22)$$

The constant  $v_\infty$  is the asymptotic [ $R(t) \rightarrow \infty$ ] velocity of a loop, and depends (for given  $D$  and  $\eta$ ) only on the function  $\tilde{f}(L)$  and its chosen pair of minima.

Our numerical analyses of the original two-dimensional equation (18), starting from initial trial profiles mimicking the expected kink structure, show that both the kink shape  $\Phi$  in the moving coordinate frame and the right-hand side of Eq. (22) remain practically constant as the kink moves. Thus, while the results to be reported in Sec. IV C are all obtained from the numerical solution of Eq. (18), the one-dimensional mapping described above usually is an excellent approximation and provides, as discussed next, a useful framework for interpreting the results.

The critical loop radius  $R_c$  corresponds to that value of  $R$  for which  $dR/dt = 0$ . From Eq. (22), this yields the relationship between  $R_c$  and  $v_\infty$ ,

$$R_c = \frac{D}{\eta v_\infty}. \quad (23)$$

Using Eq. (16), this becomes

$$R_c = \frac{E}{\tilde{f}(L_2) - \tilde{f}(L_1)}. \quad (24)$$

One recognizes that this relation is consistent with standard arguments of nucleation theory. On approximating the integrand in Eq. (20) by the constant  $\tilde{f}(L_1) - \tilde{f}(L_2)$  inside a circle of radius  $R - \Delta R/2$ , neglecting the integrand for  $r_\perp > R + \Delta R/2$ , and using Eq. (15) within the kink region of width  $\Delta R$ , one finds for  $\Delta R \ll R$  that the free-energy change is given by the standard parabolic form [23]

$$\Delta F = -\pi R^2 [\tilde{f}(L_2) - \tilde{f}(L_1)] + 2\pi RE. \quad (25)$$

The first term in Eq. (25) is the decrease in film free energy due to the difference  $\tilde{f}(L_2) - \tilde{f}(L_1)$  [36] while the second term is the free energy that has to be overcome due to the line tension of the loop. Maximizing  $\Delta F$  with respect to  $R$  yields the critical radius  $R_c$  given by Eq. (24). The corresponding activation free energy  $F_{act} = \Delta F(R_c)$  is

$$F_{act} = \frac{\pi E^2}{\tilde{f}(L_2) - \tilde{f}(L_1)} = \pi R_c E. \quad (26)$$

The expression for  $E$  given earlier in Eq. (17) agrees with a familiar mean-field relation for the tension of a stationary interface in terms of its profile shape [37]. Here that relation also applies to a moving kink of sufficiently large radius, under the assumption (supported by our numerical studies) that the profile shape is preserved during its motion.

One final point to note concerns the physical interpretation of the equation of motion Eq. (22) for  $R(t)$ . This equation is equivalent to the balance of thermodynamic and dissipative forces per unit length of the dislocation line,

$$\frac{1}{2\pi R} \left( \frac{d\Delta F}{dR} \right) + \eta \frac{E}{D} \left( \frac{dR}{dt} \right) = 0. \quad (27)$$

This yields Eq. (22) on using Eqs. (16) and (25), and agrees with the model of dislocation-loop dynamics described by Geminard *et al.* [21], on identifying the mobility  $\mu$  used by these authors with the quantity  $Dd/(\eta E)$ . Note that if  $v_\infty$  is known, then  $R(t)$  at an arbitrary time can be found by solving Eq. (22) [35], which gives the relation

$$t - t_0 = \frac{1}{v_\infty} \int_{R_0}^R \frac{dR'}{R' - R_c} \frac{R'}{R' - R_c} = \frac{1}{v_\infty} \left( R - R_0 + R_c \ln \left| \frac{R - R_c}{R_0 - R_c} \right| \right), \quad (28)$$

where  $R_0$  is the radius at an arbitrary initial time  $t_0$ . The study of dislocation-loop dynamics in Ref. [21], performed below the bulk  $A$ - $N$  transition temperature, showed that Eq. (28) very well fits experimental data. Performing our own fit of Eq. (28) to the data reported in Ref. [21] yields the values  $v_\infty = 2.59 \mu\text{m/s}$  and  $R_c = 42.6 \mu\text{m}$ , to be contrasted with results described below for overheated films.

### C. Numerical results

Figure 5 illustrates the dependence of the free energy  $\Delta F$  on radius  $R$  due to a growing dislocation loop in a six-layer film, for the case of  $f(L)$  shown in Fig. 1 and  $\Delta P = 0$ . The in-plane distance is expressed in units of  $R_{sc} \equiv d\sqrt{Dd/C}$ , as in Fig. 2, while the free energy is plotted in units of  $Dd^2$ , which follows by scaling of Eq. (20). The crosses are obtained by evaluating Eq. (20) while monitoring the numerical solution of Eq. (18) for a dynamically stable kink as it evolves with time, where the loop radius  $R$  is defined such that  $L(R) = [L(0) + L(\infty)]/2$ . It is seen that  $\Delta F(R)$  is very well fit by Eq. (25): the fitted value of  $f(L_2) - f(L_1)$  agrees with that obtained directly from the static theory with a precision of 0.5%. We also verified that the right-hand side of Eq. (22) remains constant within the same precision, giving a

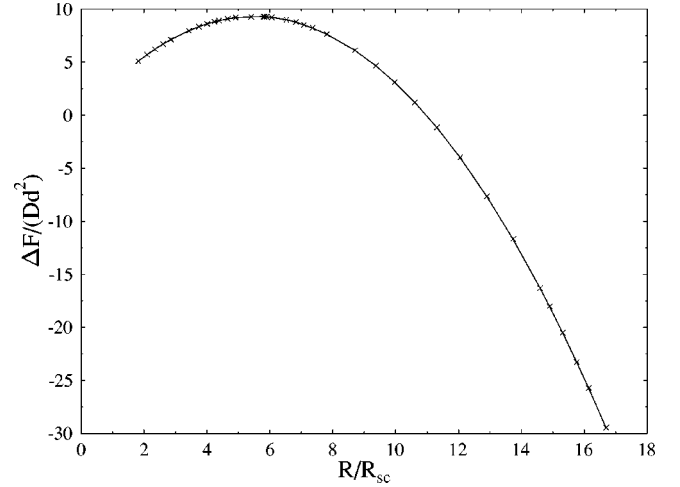


FIG. 5. Free energy  $\Delta F$  (reduced by  $Dd^2$ ) of a dislocation loop in a 6-layer film vs radius  $R/R_{sc}$ . Crosses: numerical results obtained from Eq. (20) and the solution of the dynamical equation Eq. (18) for the same  $f(L)$  and  $r_s$ -model parameters as in Fig. 1, with  $\Delta P = 0$ . Solid line: fit of  $\Delta F$  with the parabolic function in Eq. (25). The best fit yields  $E = 0.54\sqrt{DCd}$  and  $\tilde{f}(L_2) - \tilde{f}(L_1) = 0.098C/d$ .

value  $v_\infty = 0.18D/(\eta R_{sc})$ . This numerical calculation supports the ansatz Eq. (21) for a two-dimensional kink with constant  $v_\infty$  related to  $R(t)$  by Eq. (22). Analogous fittings to Eqs. (25) and (22) of the numerically determined  $\Delta F(R)$  and kink radius have been carried out for all our calculations, showing comparable precision except very close to the maximum temperature of an  $N$ -layer film, where uniform thinning is found to occur. As a further check, we find very close agreement between the values of the line tension  $E$  obtained from the fitting to Eq. (25) and by direct evaluation of Eq. (17) using the numerically determined kink profiles.

Only recently, in Ref. [13], have the dynamics of dislocation loops in overheated films been studied experimentally, albeit for a system exhibiting a *first-order* bulk  $A$ -isotropic ( $I$ ) transition. (This difference will be discussed in Sec. V.) The magnitude of the loop velocity was found to be  $10^3 - 10^4$  times larger than that reported for the smectic- $A$  phase in Ref. [21], which we will comment on further below. We note that the data in Ref. [13] show a purely linear dependence of  $R$  on time, suggesting that  $R/R_c \gg 1$  in the experimentally accessible range and that the measured velocity corresponds to  $v_\infty$  of the present theory. The data reported in Ref. [13] also show that the dislocation-loop velocity slightly increases with increasing number of layers. To check the dependence of  $v_\infty$  on thickness in our theory we took  $\eta$  to be independent of  $N$ . Figure 6 shows the results of calculations using the  $f(L)$  function employed in Fig. 1. It is seen that in some range of thickness the velocity slightly increases with  $N$  provided that  $\Delta P > 0$ . We do not rule out that  $\eta$  depends on thickness and diminishes with  $N$ , as suggested in Ref. [13], but a detailed analysis of  $\eta$  is beyond the scope of this paper. Figure 7 shows, in the case of a five-layer film, that  $v_\infty$  is predicted to increase with temperature, in agreement with experiment [13]. The rate of increase is enhanced in the presence of a nonzero  $\Delta P$ . The upper temperature limits of the curves in Fig. 7 are slightly less than the maximum tempera-

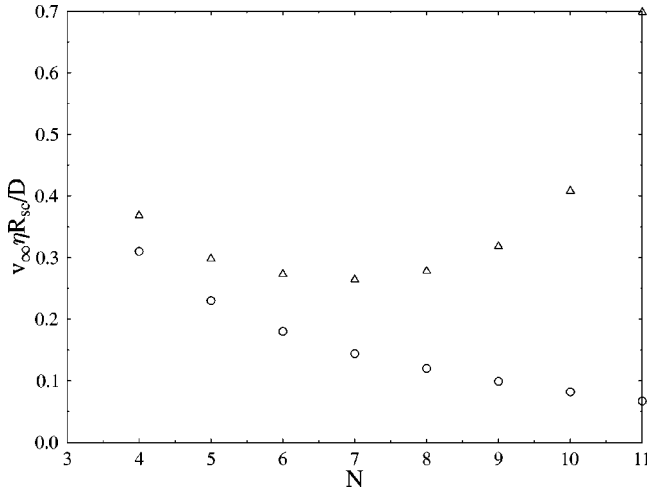


FIG. 6. Velocity  $v_\infty$  [reduced by  $D/(\eta R_{sc})$ ] for  $N$ -layer films vs the number of layers, calculated using the  $f(L)$  depicted in Fig. 1. Circles:  $\Delta P=0$ . Triangles:  $\Delta P=0.05C/d^2$  (as in Fig. 2).

tures for the given values of  $N$  and  $\Delta P$ . Beyond these limits, we find that dislocation-loop growth is superceded by uniform thinning.

Using Eq. (23) and the velocity data in Fig. 6, the critical radius  $R_c$  can be determined. Referring only to the points for  $N=11$  in the figure, we find that  $R_c=14.9R_{sc}$  and  $1.43R_{sc}$  for  $\Delta P=0$  and  $\Delta P=0.05C/d^2$ , respectively. These values bracket the range of  $R_c$  values obtained for other values of  $N$ . Using the estimate for  $R_{sc}$  described at the end of Sec. III, we thus find  $R_c$  to be in the range  $10^{-1}$  to  $10^{-2}$   $\mu\text{m}$ , several orders of magnitude lesser than the value deduced at the end of the preceding subsection in the bulk smectic- $A$  phase. In view of Eq. (23), these results are consistent with the reported differences in loop velocity  $v_\infty$  below and above the bulk transition temperature.

The key quantity that determines whether spontaneous nucleation of a dislocation loop in an overheated film actually occurs is the activation free energy  $F_{act}$ . The depen-

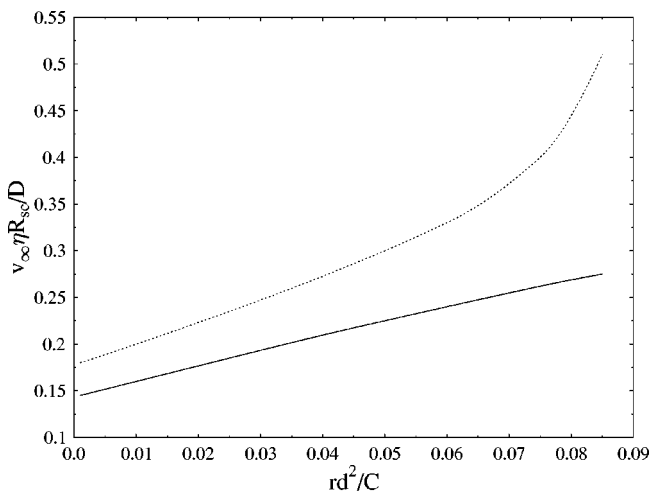


FIG. 7. Reduced velocity for a five-layer film vs  $rd^2/C \propto (T - T^*)$ . Parameters of the  $r_s$  model are the same as in Fig. 1. Lower curve (solid):  $\Delta P=0$ . Upper curve (dashed):  $\Delta P=0.05C/d^2$ .

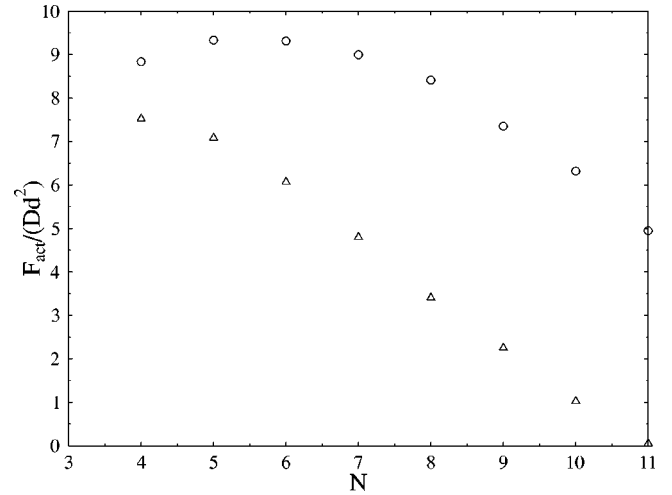


FIG. 8. Activation free energy  $F_{act}$  (reduced by  $Dd^2$ ) for  $N$ -layer films vs the number of layers calculated using the  $f(L)$  function shown in Fig. 1. Circles:  $\Delta P=0$ , triangles:  $\Delta P=0.05C/d^2$ .

dence of the reduced  $F_{act}$  for a single-layer dislocation loop on the number of layers  $N$  in the initial uniform film, is shown in Fig. 8. Again, the calculations were done using the  $f(L)$  function depicted in Fig. 1. Note that the temperature in this case is slightly below the maximum temperature for an 11-layer film. To judge whether nucleation occurs, we use the argument described in Ref. [12], based on the frequency per unit area of forming a dislocation loop of radius  $R > R_c$ . This frequency is given by  $f=f_0 \exp(-F_{act}/k_B T)$ , where  $f_0$  is estimated to be  $10^{26} \text{ cm}^{-2} \text{ s}^{-1}$  [23]. As shown in Ref. [12], this gives that the condition for a dislocation loop to nucleate in 0.1 s in a 1-cm<sup>2</sup> film is  $F_{act}/k_B T \approx 60$ . To compare this number with Fig. 8 requires a value for the dimensionless parameter  $Dd^2/(k_B T)$ . Taking  $D=\gamma/2 \approx 1.5 \times 10^{-2}$  N/m,  $k_B T=4.5 \times 10^{-21}$  J, and  $d=3 \times 10^{-9}$  m, we estimate that  $Dd^2/k_B T \approx 30$ . These numbers yield the criterion that  $F_{act}/(Dd^2)$  must become about 2 or smaller for spontaneous nucleation to occur. Figure 8 shows that, for the chosen set of parameters, this can be achieved provided that  $\Delta P > 0$  is sufficiently large.

Figure 9 shows the variation of the line tension  $E$  with initial number of layers  $N$  for the same cases shown in Figs. 6 and 8. Except for the last two points in the figure ( $N=10,11$ ),  $E$  is seen to be essentially independent of  $\Delta P$ . It follows from Eq. (26) that it is the decreasing magnitude of  $E$  on approaching  $N_{cr}$  for a given  $T$  that is mainly responsible for the decrease in  $F_{act}$  in Fig. 8 near  $N_{cr}$  and, similarly, for the increase of  $v_\infty$  when  $\Delta P > 0$  in Fig. 6. The difference between the two cases shown in Figs. 6 and 8, for  $\Delta P=0$  and  $\Delta P > 0$ , is due to the fact that  $\tilde{f}(L_2) - \tilde{f}(L_1) \approx f(L_2) - f(L_1) + \Delta P d$  is dominated by the term  $\Delta P d$  in the latter case for the value of  $\Delta P$  used.

## V. CONCLUSIONS

The present theory, a modification of de Gennes' [15] theory of presmectic films, is based on the generally ac-

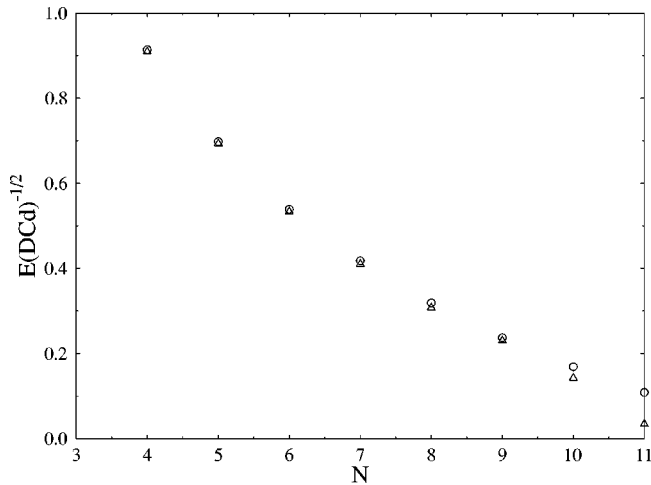


FIG. 9. Line tension  $E$  (reduced by  $\sqrt{DCd}$ ) for  $N$ -layer films vs the number of layers, calculated using  $f(L)$  depicted in Fig. 1. Circles:  $\Delta P=0$ , triangles:  $\Delta P=0.05C/d^2$ .

cepted view [12] that the occurrence of overheated free-standing films is due to surface-enhanced smectic ordering [7]. In the case of a uniform planar film, our theory [11] predicts that there is a maximum temperature for which smectic ordering in an  $N$ -layer film can occur. We associate this with an upper bound for the true layer-thinning transition temperature  $T_c(N)$ . Employing a dynamical generalization of the theory based on a TDGL equation, we have shown that thinning via nucleation of dislocation loops, the mechanism indicated by recent experiments [12–14], is possible provided the pressure difference  $\Delta P$  resulting from curvature of the surrounding meniscus is sufficiently large. Otherwise, the film would undergo either “uniform thinning” or, possibly, rupturing by a process analogous to spinodal dewetting [30]. The requirement for a nonzero  $\Delta P$  to promote nucleation of dislocation loops is consistent with other recent studies [10,14], although we emphasize here that the condition  $\Delta P \neq 0$  is not essential for *some* type of thinning process to occur.

In the present paper, all nucleation properties (i.e.,  $R_c, F_{act}, v_\infty, E$ ) are interrelated within the framework of solutions to the TDGL equation. In particular, the line tension  $E$  of the dislocation loop is expressed in terms of the kink profile, see Eq. (17). From this equation,  $E$  depends self-consistently on the elastic behavior of the system through the dependence of the kink shape on the uniform-film free en-

ergy  $\tilde{f}(L)$  and via possible elastic effects contained (see Sec. III) in the coefficient  $D$ . In contrast, previous related works [10,12,14,21] have evaluated nucleation properties using estimates for the line tension  $E$  obtained from independent analyses, rather than being related self-consistently to the kink shape.

It is important to emphasize that the present paper is restricted to smectic- $A$  liquids undergoing continuous  $A$ - $N$  transitions in bulk. For this reason we do not attempt to make quantitative comparisons with the experimental results of Ref. [13] for dislocation-loop dynamics, since the latter pertain to a system with a first-order  $A$ - $I$  transition. Such a system can be treated using the present Landau-de Gennes theory (albeit with considerably greater complexity) by appropriately modifying the bulk free-energy density in Eq. (2). One significant difference that is expected concerns contributions to the “ $\Delta P$ ” term in the resulting uniform-film free energy. In a system with a first-order bulk transition, such a term arises even in the absence of meniscus effects, due to the grand-canonical [17] free-energy difference between a *metastable* bulk smectic- $A$  phase and the isotropic phase [9,18]. This effect was recognized in the nucleation theory of Ref. [12], although the latter work otherwise employed de Gennes’ theory for a second-order bulk transition. Clearly, to compare the present dynamical predictions with experiment, it would be of interest to perform measurements on the dynamics of layer thinning in systems such as that studied in Ref. [14], which exhibit second-order bulk  $A$ - $N$  transitions.

Our picture is that dislocation-mediated thinning of an overheated free-standing smectic film may preempt the uniform-thinning mechanism and thus, for given  $N$  and fixed values of the model parameters such as  $r_s$ , occur at a lower temperature than predicted [11] by considering a purely uniform film. This is conceivable because *all* free-standing film states are metastable [18]. Here we have presented several qualitative results in support of this picture. An additional step would be to evaluate the shift in layer-thinning transition temperatures  $T_c(N)$  from those predicted [11] for a uniform film, and attempt a refitting with experimental data, a task left for future study. Further studies will also be directed to evaluating the kinetic coefficient  $\eta$  and, as already mentioned, extending the present theory to smectic films with first-order bulk transitions.

## ACKNOWLEDGMENTS

This study was supported by the Natural Sciences and Engineering Research Council (Canada).

- [1] T. Stoebe, P. Mach, and C. C. Huang, Phys. Rev. Lett. **73**, 1384 (1994).
- [2] P. M. Johnson *et al.*, Phys. Rev. E **55**, 4386 (1997).
- [3] S. Pankratz, P. M. Johnson, H. T. Nguyen, and C. C. Huang, Phys. Rev. E **58**, R2721 (1998).
- [4] E. I. Demikhov, V. K. Dolganov, and K. P. Meletov, Phys. Rev. E **52**, R1285 (1995).
- [5] E. A. L. Mol *et al.*, Physica B **248**, 191 (1998).
- [6] P. Cluzeau *et al.*, Phys. Rev. E **62**, R5899 (2000). This work

- describes observations of layer-thinning transitions in a smectic- $C$  liquid crystal.
- [7] C. Bahr, Int. J. Mod. Phys. B **8**, 3051 (1994).
- [8] L. V. Mirantsev, Liq. Cryst. **20**, 417 (1996).
- [9] Y. Martinez-Raton, A. M. Somoza, L. Mederos, and D. E. Sullivan, Faraday Discuss. **104**, 111 (1996); Phys. Rev. E **55**, 2030 (1997).
- [10] E. E. Gorodetskii, E. S. Pikina, and V. E. Podnek, Zh. Eksp. Teor. Fiz **115**, 61 (1999) [JETP **88**, 35 (1999)].

- [11] A. N. Shalaginov and D. E. Sullivan, *Phys. Rev. E* **63**, 031704 (2001).
- [12] S. Pankratz, P. M. Johnson, R. Holyst, and C. C. Huang, *Phys. Rev. E* **60**, R2456 (1999).
- [13] S. Pankratz, P. M. Johnson, A. Paulson, and C. C. Huang, *Phys. Rev. E* **61**, 6689 (2000).
- [14] F. Picano, P. Oswald, and E. Kats, *Phys. Rev. E* **63**, 021705 (2001).
- [15] P. G. de Gennes, *Langmuir* **6**, 1448 (1990).
- [16] D. E. Sullivan and M. M. Telo da Gama, in *Fluid Interfacial Phenomena*, edited by C. A. Croxton (Wiley, New York, 1986), p. 45; M. Schick, in *Les Houches, Session XLVIII, 1988—Liquides aux Interfaces*, edited by J. Charvolin, J. F. Joanny, and J. Zinn-Justin, (Elsevier, New York, 1990), p. 418.
- [17] As appropriate for an open system, the film free energy in Eq. (2) is really the excess grand canonical potential per unit area: see Ref. [18]. Note that Eq. (2) only involves the effects of smectic ordering, and omits the contribution to the free energy of a background isotropic density variation across the film, which is assumed to be constant.
- [18] Y. Martinez, A. M. Somoza, L. Mederos, and D. E. Sullivan, *Phys. Rev. E* **53**, 2466 (1996).
- [19] M. E. Fisher, in *Statistical Mechanics of Membranes and Surfaces*, edited by D. Nelson, T. Piran, and S. Weinberg (World Scientific, Singapore, 1989), p. 19.
- [20] The surface contribution to the film free energy in Ref. [14] (see also Refs. [21] and [22]) is of the more general form  $2\gamma([1 + (\nabla_{\perp} L)^2/4]^{1/2} - 1)$ .
- [21] J. C. Geminard, R. Holyst, and P. Oswald, *Phys. Rev. Lett.* **78**, 1924 (1997).
- [22] F. Picano, R. Holyst, and P. Oswald, *Phys. Rev. E* **62**, 3747 (2000).
- [23] P. G. de Gennes and J. Prost, *The Physics of Liquid Crystals* (Clarendon Press, Oxford, 1993); *Adv. Phys.* **33**, 1 (1984).
- [24] B. V. Toshev and I. B. Ivanov, *Colloid Polym. Sci.* **253**, 558 (1975).
- [25] P. Pieranski *et al.*, *Physica A* **194**, 364 (1993).
- [26] S. A. Safran, *Statistical Thermodynamics of Surfaces, Interfaces, and Membranes* (Addison-Wesley, Reading, 1994), Chap. 4.
- [27] L. M. Pismen and Y. Pomeau, *Phys. Rev. E* **62**, 2480 (2000).
- [28] J. A. de Feijter, in *Thin Liquid Films, Fundamentals and Applications*, edited by I. B. Ivanov (Dekker, New York, 1988), p. 1.
- [29] A. J. Bray, *Adv. Phys.* **43**, 357 (1994).
- [30] The solution of Eq. (11) at the maximum temperature when  $\Delta P = 0$  differs from that for  $\Delta P > 0$ . Since  $\partial \tilde{f} / \partial L = 0$  at the initial film thickness  $L_0$ , there is no *uniform* nonstationary solution of Eq. (11) when  $\Delta P = 0$ . Numerically determined solutions for moving kinks (Sec. IV B) in this case exhibit a divergent kink width. A related effect is a long-range decay of the meniscus profile obtained from Eq. (6). Fluctuations omitted here are probably important in this situation, e.g., leading to film rupture or thinning by spinodal decomposition.
- [31] W. van Saarloos, *Phys. Rev. A* **37**, 211 (1988).
- [32] M. Buttiker and H. Thomas, *Phys. Rev. A* **37**, 235 (1988).
- [33] V. Popa-Nita and T. J. Sluckin, *J. Phys. II* **6**, 873 (1996).
- [34] A. N. Shalaginov, L. D. Hazelwood, and T. J. Sluckin, *Phys. Rev. E* **60**, 4199 (1999).
- [35] S. Chan, *J. Chem. Phys.* **67**, 5755 (1977).
- [36] Note that in other works [10,12,14], the quantity  $\tilde{f}(L_2) - \tilde{f}(L_1)$  in Eqs. (24)–(26) has been approximated from the outset by  $\Delta P d$ . This should be valid well in the smectic-A phase, where the minima of  $f(L)$  are expected to be nearly equal, but is not generally true in the overheated regime.
- [37] P. M. Chaikin and T. C. Lubensky, *Principles of Condensed Matter Physics* (Cambridge University Press, Cambridge, U.K., 1995).